Water as a molecular hinge in amide-like structures

R. L. A. Timmer* and H. J. Bakker

FOM-institute for Atomic and Molecular Physics,

Kruislaan 407, 1098 SJ Amsterdam, The Netherlands

Abstract

We have studied the reorientational dynamics of isolated water molecules in a solution of N,N-Dimethylacetamide (DMA). From linear spectra, we find that the water in this solution forms double hydrogen bond connections to the DMA molecules resulting in the formation of DMA-water-DMA complexes. We use polarization-resolved mid-infrared pump-probe spectroscopy on the water in these complexes to measure the depolarization of three distinct transition dipole moments, each with a different directionality relative to the molecular frame (OH-stretch in HDO, symmetric and asymmetric stretch normal modes in H_2O). By combining these measurements, we find that the system exhibits bimodal rotational dynamics with two distinct timescales: a slow (7±1 ps) reorientation of the entire DMA-water complex and a fast (0.5±0.2 ps) 'hinging' motion of the water molecule around the axis parallel to the connecting hydrogen bonds. Additionally, we observe an exchange of energy between the two normal modes of H_2O at a timescale of 0.8±0.1 ps and find that the vibrational excitation decays through the symmetric stretch normal mode with a time constant of 0.8±0.2 ps.

I. INTRODUCTION

Water plays an important role in a wide variety of chemical interactions. Many of its distinct properties stem from the polar nature of the water molecule and its ability to form hydrogen bonds with up to four neighboring water molecules. In bulk water this behavior causes it to form large interconnecting networks resulting in rapid exchange and delocalization of energy and charges. Water can act as a mediator in proton transfer such as those occurring in acid-base reactions[1] or as an essential component in the formation and interaction of certain (bio)molecules[2].

Protein structure and stability are governed in large part by hydrophobic collapse and hydrophilic interactions with water. Single embedded water molecules can form bridges between oxygen atoms of different amide groups through double hydrogen bond formation[3]. In this way they can hold together bio-molecular chains and assist in the formation of tertiary structures. Functionally, water plays an important role as a reactant at active sites or in molecular recognition through the unique directionality and adaptability of its hydrogen bonds[4]. It is clear that these bridging water molecules play an essential biological role and their properties must be carefully considered when studying the functional implications of protein structures.

A technique well suited for the study of water on the sub-picosecond timescale is polarization-resolved mid-infrared pump-probe spectroscopy[5–10]. Using this technique, more insight was gained, recently, into the dynamics of water hydrogen bonded to molecules such as acetone[11], acetonitrile[12], DMSO[13], and urea[14]. These studies have helped to quantify many interesting properties such as (vibrational) energy transfer rates and rotational diffusion dynamics.

The goal of this study is to model the molecular motions and energy dynamics that are exhibited by single water molecules bridged between two amide groups. As a model system we use a dilute solution of water dissolved in N,N-Dimethylacetamide (DMA). DMA possesses the same characteristic O=C–N group that is present in amides. The N–H groups have been replaced by amino-methyl groups (N–CH_3) to avoid spectral interference of the NH-stretching frequency on our measurements of the OH-stretching frequency of water. This replacement is expected to have negligible effects on the hydrogen bonding to the oxygen atom. By combining measurements of normal and partially deuterated water, we are able to

deduce the three-dimensional rotational behavior of these water molecules as well as their energy transfer dynamics.

II. EXPERIMENT

A. Laser setup

The experiment consisted of a polarization-resolved two-color pump-probe setup with the following characteristics. A commercial titanium-sapphire laser system ('Titan') generated 150 femtosecond pulses, at a wavelength of 800 nanometer and an energy of about 2.5 mJ at a repetition rate of 1 kHz. These pulses were split into three equal parts. Two parts were used to pump two separate β barium borate (BBO) based OPAs. Idler pulses coming from the first OPA were frequency doubled in a BBO-crystal to a wavelength of about 1100 nm and then combined with the third part of the 800 nm beam in a $KTiOPO_4$ (KTP) crystal to yield strong (5 μJ) narrow band pump pulses with a center frequency tunable between 3450 and 3550 cm^{-1} and a FWHM of 100 cm^{-1}. Signal and idler pulses coming from the second OPA were difference frequency mixed in a crystal of $AgGaS_2$ to create low-energy (20 nJ) broadband probe pulses at about 3500 cm^{-1} with a FWHM of 250 cm^{-1}.

The probe beam was split into two beams by reflection off a CaF_2 wedged window, referred to as signal and reference. Both beams were sent through the sample, but only the signal beam was overlapped with the pump beam. The delay time between pump and probe was varied by means of a delay stage with a resolution of about 0.03 ps. The spatially overlapping pump and signal beams hit the sample with a relative difference in polarization angle of 45 degrees. After the sample, the signal beam was sent onto a home-built rotating polarizer, which alternately selected between the signal components parallel and perpendicular to the pump beam. The signal and reference beams were frequency resolved by a spectrometer and detected by two 32-pixel Mercury Cadmium Telluride (MCT) arrays. The signal was normalized by the reference beam to filter out intensity fluctuations in the individual laser pulses. The pump beam was chopped with a frequency of 500 Hz to provide alternating pumped and unpumped absorption spectra for the probe. The instrument response time was about 200 fs.

B. Polarization-resolved pump-probe spectroscopy

In our experiments, we measure the pump-induced frequency-resolved absorption differences in a sample. The resulting transient absorption spectra ($\nu = 0 \rightarrow 1$ bleach and $\nu = 1 \rightarrow 2$ induced absorption) are measured as a function of time delay between pump and probe, thus revealing the temporal evolution of the different states. To calculate the absorption changes ($\Delta\alpha$) induced by the pump beam, probe transmissions through the sample with (T) and without (T_0) pump are compared :

$$\Delta\alpha(t,\nu) = -\ln(T(t,\nu)/T_0(\nu)) \tag{1}$$

The absorption cross section is proportional to the directional overlap between the transition dipole of the absorbing oscillator and the polarization of the light. This means that the pump beam, which is linearly polarized, will induce an anisotropic population of excited oscillators in the sample, preferentially parallel to the pump polarization. This anisotropy can be probed with a set of probe beams, one parallel and one perpendicular to the pump. The absorption of the parallel and perpendicular probe beams are used to construct the isotropic signal $\Delta\alpha_{iso}(t,\nu)$ and the anisotropy $R(t,\nu)$:

$$\Delta\alpha_{iso}(t,\nu) = \frac{\Delta\alpha_{\parallel}(t,\nu) + 2\cdot\Delta\alpha_{\perp}(t,\nu)}{3} \tag{2}$$

$$R(t,\nu) = \frac{\Delta\alpha_{\parallel}(t,\nu) - \Delta\alpha_{\perp}(t,\nu)}{\Delta\alpha_{\parallel}(t,\nu) + 2\cdot\Delta\alpha_{\perp}(t,\nu)} \tag{3}$$

The isotropic signal depends only on the vibrational relaxation and is independent of reorientational motion. Conversely, the anisotropy is purely dependent on the reorientational motion and is proportional to the auto-correlation function of the direction of the excited transition dipole moment, as:

$$R(t) = \frac{2}{5}\langle P_2(\hat{\mu}(0)\cdot\hat{\mu}(t))\rangle \tag{4}$$

where $\hat{\mu}(0)\cdot\hat{\mu}(t)$ is the inner product between unit vectors along the direction of transition dipole moments at times 0 and t. P_2 is the second Legendre polynomial and $\langle ...\rangle$ denotes the ensemble average.

From the anisotropy decay curves, we obtain information about the average reorientational motions of the pumped dipole oscillators. Here we study three distinct transition dipole moments of the water molecule (symmetric, asymmetric and single OH). As is shown

in figure 1, these three modes have different directions of their transition dipole moments. The symmetric and asymmetric vibrational stretch modes of H_2O are orthogonal with respect to each other and have angles of 52 and 38° with respect to the OH vibration of HDO, which is directed parallel to the stretching motion of the OH oscillator. By combining the anisotropy decay data from these three modes we can identify the rotational motions of the embedded water molecules. The differences in anisotropy decay of the three modes will reveal the preferred direction(s) of reorientation. Furthermore, when the anisotropy of one or more modes does not decay back to zero, this implies that the orientation of the water molecule retains some long lasting, correlated direction with respect to its initial 'pumped' direction.

C. Samples under study

To study the vibrational and orientational dynamics of water in amide-like structures, we used two different samples. The first sample consisted of a mixture of HDO in D_2O (with a tiny fraction H_2O), dissolved in N,N-Dimethylacetamide (DMA). It was produced by mixing DMA, D_2O and H_2O with molar ratios DMA:D_2O:H_2O = 100:20:3. This sample is subsequently referred to as DMA-HDO.

The second sample consisted of a solution of pure H_2O in DMA, with molar ratios DMA:H_2O = 100:3. This sample is subsequently referred to as DMA-H_2O. Both samples were contained in a static sample cell with an optical path length of 100 μm.

A recent study on the structure of aqueous mixtures in DMA by Nishi et al.[15] showed that for molar fractions of DMA > 0.6, DMA clusters are dominant and very few (if any) water clusters remain. The experiments presented here were performed on samples with DMA molar fractions > 0.8 so that we can safely assume that we were dealing with isolated water molecules.

III. RESULTS

A. Linear spectra

To isolate the absorption cross section of OH-oscillators in DMA-HDO and DMA-H_2O, we subtract reference samples consisting of the same constituents but without H_2O. For

DMA-HDO, this is a mixture of DMA:D_2O with molar ratios 100:20 and for DMA-H_2O, this is a pure DMA sample. Figure 2 shows the linear absorption spectra of DMA-HDO and DMA-H_2O, with the absorption of the reference samples subtracted. This means that the absorptions, shown here, are only due to the OH-oscillators in the sample. The subtracted background consists mainly of the absorption bands of DMA and overtone bands of D_2O. These bands have a much lower absorption cross-section than that of the OH oscillator but are presents due to their large excess in the sample. We can safely neglect this background in our pump-probe measurements because the pump-probe signal depends quadratically on the absorption cross-section.

The dashed line spectrum in figure 2 is that of HDO in DMA. It consists of a main absorption band, with a central frequency around 3460 cm^{-1}. The shape is slightly asymmetric, absorbing more strongly at lower frequencies. In addition to the OH-stretching mode, shown here, HDO also has an OD-stretching mode at a much lower frequency ($\sim$2550 cm^{-1}). Because the two frequencies are far apart, the mixing of these modes is minimal. Consequently in HDO it is possible to excite either the local OD or the local OH oscillator. The latter will subsequently be referred to as mode H (see fig. 1).

When we compare the solid line spectrum of H_2O in DMA with that of HDO we find that there are *two* main absorption bands as opposed to one. Doubly hydrogen bonded H_2O has two equivalent OH-oscillators, that have the same reduced mass and experience similar potentials. These oscillators are strongly coupled and form two normal modes: symmetric and asymmetric, subsequently referred to as modes S and A (see fig. 1). The S mode corresponds to the lower frequency peak in the spectrum and the A mode to the higher frequency peak. As we will see in the pump-probe experimental data, S and A are not pure normal modes but are anharmonically coupled by higher order terms in the vibrational potential, resulting in the exchange of vibrational energy.

A final important thing to note is the *absence* of a free OH-oscillator peak in these spectra which would normally be around 3670 cm^{-1}. This peak *does* show up if an apolar solvent, like carbon-tetra-chloride is added to the mixture (not shown here). The absence of this 'free' peak and the large excess of DMA over water leads us to conclude that all water molecules are doubly hydrogen bonded and form structures such as depicted in figure 3.

B. Nonlinear spectra

Three different pump-probe data sets were recorded. The first is on a sample of DMA-HDO pumped at the frequency of mode H (3460 cm^{-1}). The second and third are both on DMA-H_2O, with the pump set to the frequencies of modes S (3450 cm^{-1}) and A (3550 cm^{-1}), respectively. For all samples we observe bleaching of the OH stretch absorption bands and induced absorption at lower frequencies corresponding to $\nu = 1 \rightarrow 2$ transitions. In figures 4, 5 and 6 we show the bleaching parts of these spectra.

Upon inspection of the DMA-HDO data set, shown in figure 4, we note that its isotropic part can be described by an exponentially decaying, single spectrum, corresponding to the decay of $\nu = 1_H$ (first excited state of mode H). We observe no significant contribution of spectral diffusion (i.e. changes in spectral shape) for delays > 0.4 ps. The anisotropy is independent of frequency over the presented range and can be described by a single exponential, decaying towards a non-zero end-level. This end-level is an indication that the water molecule is not able to reorient freely but retains 'memory' of its initial pumped direction for times > 10 ps.

Next, we compare the two data sets of DMA-H_2O shown in figures 5 and 6. The isotropic parts (top) display dynamics which indicate the presence of two underlying spectra, the amplitudes of which relate to the occupation of $\nu = 1_S$ and $\nu = 1_A$ (first excited states of modes S and A). These two experiments differ in the frequency (and power) of the pump beam and thus in the relative initial degree of excitation of the levels. In figure 5, $\nu = 1_S$ was initially predominantly excited and in figure 6, $\nu = 1_A$. Both experiments show a rapid exchange of energy between the normal modes, towards an equilibrium distribution, which looks similar to the linear spectrum. The equilibration is followed by a decay to zero.

In both figures 5 and 6 the anisotropy at the pump-frequency starts at a value of about 0.4, which is expected for $\hat{\mu}(0) \cdot \hat{\mu}(t) = 1$ (see eqn. (4)). However, at the frequency corresponding to the mode that was not initially pumped we find a significantly lower initial anisotropy. In the case of pumping the A mode (fig. 6), we even see a negative anisotropy at frequencies corresponding to the S mode. This negative anisotropy shows that the two normal modes exchange vibrational energy. Because the modes have *perpendicular* transition dipole moments (shown in fig. 1), every time a pumped mode S is converted to A and vice versa, the transition dipole moment is rotated over an angle of 90°. If we substitute

$\hat{\mu}(0)\cdot\hat{\mu}(t)$=0 in equation (4), we obtain a value of -0.2 for the anisotropy resulting from such a transfer. In the other data set, where the pump was set to mode S (fig. 5), the initial anisotropy at mode A is higher than -0.2 because this anisotropy also contains a contribution of oscillators that are directly pumped in the A mode (which have an initial anisotropy of 0.4). Apparently, the pump pulse spectrum centered at the S mode overlaps with the low frequency wing of the spectrum of the A mode.

A final important observation is, that the anisotropy shows a much slower decay for the directly pumped A mode than for the directly pumped S mode. This suggests that the water molecules reorient in a way that maintains the direction of the transition dipole moment of A and not that of S. A compelling explanation for these observations is an anisotropic reorientation that prefers rotations around an axis, parallel to the transition dipole moment of A. This leads to a picture in which the water molecule hinges around its two hydrogen bonds with DMA molecules, while the complex as a whole displays a much slower reorientation (see fig. 7, left). This interpretation is also consistent with the slow anisotropy decay of the indirectly pumped population of both S and A. After transfer has occurred (from A to S or from S to A), any rotation in the plane perpendicular to the direction of A will maintain the angle of 90° between the pumped and probed transition dipole directions (see fig. 7, right). As will be shown in the following section, our experimentally observed results can be reproduced quantitatively using a model based on this mechanism.

C. Kinetic model

For a quantitative interpretation of the observations we first introduce the energy level diagrams of the two systems, DMA-HDO and DMA-H_2O in figure 8. The diagram also displays the relaxation channels of the first excited states.

For the HDO case, population is pumped into the first excited state of mode H, which can then decay to a thermalized ground state 0^* with rate k_{ho*}, and back to the original ground state 0 with rate k_{o^*o}. The occupation of levels 1_H and 0^* as a function of time, denoted $N_H(t)$ and $N_{0^*}(t)$, are described by the rate equations:

$$\frac{d}{dt}\begin{pmatrix} N_H(t) \\ N_{0^*}(t) \end{pmatrix} = \begin{bmatrix} -k_{ho^*} & 0 \\ k_{ho^*} & k_{o^*o} \end{bmatrix} \begin{pmatrix} N_H(t) \\ N_{0^*}(t) \end{pmatrix} \tag{5}$$

In the case of H_2O, population is pumped into the first excited state of either S or

A (denoted 1_S and 1_A respectively). Energy transfer between these two normal modes is governed by rate constants k_{sa} and k_{as} and the decay from levels 1_S and 1_A to thermal level 0^* by rate constants k_{so^*} and k_{ao^*}, respectively. The occupation of levels 1_S, 1_A and 0^*, denoted as $N_S(t)$, $N_A(t)$ and $N_{0^*}(t)$, is described by the rate equations:

$$\frac{d}{dt}\begin{pmatrix} N_S(t) \\ N_A(t) \\ N_{0^*}(t) \end{pmatrix} = \begin{bmatrix} (-k_{sa} - k_{so^*}) & k_{as} & 0 \\ k_{sa} & (-k_{as} - k_{ao^*}) & 0 \\ k_{so^*} & k_{ao^*} & k_{o^*o} \end{bmatrix} \begin{pmatrix} N_S(t) \\ N_A(t) \\ N_{0^*}(t) \end{pmatrix} \tag{6}$$

These rate equations are solved using the methods described in appendix A.

It is assumed that each occupied level has a characteristic associated transient spectrum. The spectra of levels 1_H, 1_S, and 1_A, denoted $\sigma_H(\nu)$, $\sigma_S(\nu)$, and $\sigma_A(\nu)$, consist of decreased absorption bands ($\Delta\alpha(\nu) < 0$), due to $\nu = 0 \rightarrow 1$ ground-state bleaching and $\nu = 1 \rightarrow 0$ stimulated emission, and increased absorption bands ($\Delta\alpha(\nu) > 0$), due to $\nu = 1 \rightarrow 2$ induced absorption. The spectra $\sigma_S(\nu)$ and $\sigma_A(\nu)$ may also include the effects of mode-to-mode coupling, i.e. the influence of excitation of the S mode on the frequency of the A mode and vice versa. The spectrum σ_{0^*} of level 0^* corresponds to a change in the linear absorption spectrum that results from heating of the sample. Rate constant k_{o^*o} corresponds to the rate at which heat dissipates away from the sample and is negligibly small, because this process happens on much longer timescales than under investigation here. Because of this, $\sigma_{0^*}(\nu)$ may be equated to the absorption difference observed on long timescales (100 ps). Hence, the population $N_{0^*}(t)$ is 0 for $t = 0$ and 1 for $t \rightarrow \infty$. From the fit, which is described later, we furthermore find that $k_{ao^*} = 0$. This implies that the predominant relaxation channel of mode A is transfer of vibrational energy to mode S, from which relaxation to 0^* occurs.

With the aforementioned assumption, that each occupied level corresponds with a single spectrum, the isotropic data (see eqn. (2)) can be described by the summed products of the time evolution of these levels and their respective spectra:

$$\Delta\alpha_{HDO,iso}(t,\nu) = N_H(t)\sigma_H(\nu) + N_{0^*}(t)\sigma_{0^*}(\nu) \tag{7}$$

$$\Delta\alpha_{H_2O,iso}(t,\nu) = N_S(t)\sigma_S(\nu) + N_A(t)\sigma_A(\nu) + N_{0^*}(t)\sigma_{0^*}(\nu) \tag{8}$$

The difference between the two data sets of DMA-H_2O is assumed to arise purely from differences in the initial occupation: $N_S(0)$ and $N_A(0)$.

D. Anisotropy modeling

A description of the anisotropy dynamics requires the inclusion of the effects of transfer and (limited) anisotropic rotations. First, we split the populations of S and A that were either excited directly by the pump or excited indirectly as a result of intramolecular transfer. Second, we break up the rotation of the water molecule into two motions (see fig. 7): reorientational diffusion D_M of the water molecule within the complex and reorientational diffusion D_C of the DMA-water complex itself. Finally, we assign end-levels to the anisotropy of the water molecule in the complex, reflecting its limited range of reorientation. We thus define the following set equations describing the temporal evolution of the anisotropies:

$$R_H(t) = [R_{f,H} + (R_{i,H} - R_{f,H}) \exp(-D_M t)] \cdot \exp(-D_C t) \tag{9}$$

$$R_{SS}(t) = [R_{f,SS} + (R_{i,SS} - R_{f,SS}) \exp(-D_M t)] \cdot \exp(-D_C t) \tag{10}$$

$$R_{SA}(t) = [R_{f,SA} + (R_{i,SA} - R_{f,SA}) \exp(-D_M t)] \cdot \exp(-D_C t) \tag{11}$$

$$R_{AS}(t) = [R_{f,AS} + (R_{i,AS} - R_{f,AS}) \exp(-D_M t)] \cdot \exp(-D_C t) \tag{12}$$

$$R_{AA}(t) = [R_{f,AA} + (R_{i,AA} - R_{f,AA}) \exp(-D_M t)] \cdot \exp(-D_C t) \tag{13}$$

Where the anisotropy of level H, in DMA-HDO, is given by $R_H(t)$. The initial and final anisotropy levels of the water molecule, in the reference frame of the complex, are given by $R_{i,H}$ and $R_{f,H}$. For the part between square brackets, these values are obtained at $t = 0$ and $t \to \infty$, respectively. This 'molecular' anisotropy, diffusing with rate D_M, is then multiplied with the anisotropy decay of the whole complex, diffusing with rate D_C. The anisotropy of levels S and A, in DMA-H_2O, is given by $R_{XY}(t)$, where X is the currently excited mode and Y is the initially excited mode (either S or A). In this way we take into account the possibility of transfer between modes. Values for $R_{i,XY}$ are 0.4 if $X = Y$ and -0.2 if $X \neq Y$. The same rotational diffusion rates, D_M and D_C, must hold for all three experiments.

Before we can determine the values of the final anisotropy levels, $R_{f,XY}$, we must make an assumption about the range of motions of the water molecules inside the complex. Because of considerations given earlier, we assume a (partially) circular motion around the axis parallel with the asymmetric stretch mode (see fig. 7). Using equation (4) with $t \to \infty$, we can evaluate some end-levels for this motion and find: $R_{f,SA} = -0.2$, $R_{f,AS} = -0.2$ and $R_{f,AA} = 0.4$. The values for $R_{f,H}$ and $R_{f,SS}$ are dependent on the angle $\Delta\phi$ over which the

molecule diffuses within the circle, as explained in appendix B. This angle will be left as a free parameter in the model, but will have to give consistent values for $R_{f,H}$ and $R_{f,SS}$.

E. Spectral shapes

By expanding equation (7) we can relate the measured values for $\Delta\alpha_{HDO,iso}(t,\nu)$, $\Delta\alpha_{HDO,\parallel}(t,\nu)$ and $\Delta\alpha_{HDO,\perp}(t,\nu)$ to the population of mode H and its corresponding anisotropy:

$$\begin{pmatrix} N_H(t) \\ N_{H,\parallel}(t) \\ N_{H,\perp}(t) \end{pmatrix} \Big(\sigma_H(\nu) \Big) = \begin{pmatrix} \Delta\alpha_{HDO,iso}(t,\nu) \\ \Delta\alpha_{HDO,\parallel}(t,\nu) \\ \Delta\alpha_{HDO,\perp}(t,\nu) \end{pmatrix} \tag{14}$$

where $\sigma_H(\nu)$ is the absorption cross-section of mode H and we have defined the parallel and perpendicular populations for mode H as

$$N_{H,\parallel}(t) \equiv [1 + 2R_H(t)] \cdot N_H(t) \tag{15}$$

$$N_{H,\perp}(t) \equiv [1 - R_H(t)] \cdot N_H(t) \tag{16}$$

respectively.

We use the kinetic model of equation 5 and the anisotropy decay from equation 9 to find values for $N_H(t)$, $N_{H,\parallel}(t)$ and $N_{H,\perp}(t)$ as a function of the parameters for energy relaxation and rotational diffusion. We thus obtain three equations that all depend on $\sigma_H(\nu)$. This matrix equation can be solved using linear regression techniques to yield the best fitting spectral shape $\sigma_H(\nu)$. The advantage of this technique is that the spectrum σ_H follows directly from the data and model parameters.

The same expansion can be done for DMA-H_2O (eqn.8) yielding

$$\begin{pmatrix} N_S(t) & N_A(t) \\ N_{S,\parallel}(t) & N_{A,\parallel}(t) \\ N_{S,\perp}(t) & N_{A,\perp}(t) \end{pmatrix} \begin{pmatrix} \sigma_S(\nu) \\ \sigma_A(\nu) \end{pmatrix} = \begin{pmatrix} \Delta\alpha_{H2O,iso}(t,\nu) \\ \Delta\alpha_{H2O,\parallel}(t,\nu) \\ \Delta\alpha_{H2O,\perp}(t,\nu) \end{pmatrix} \tag{17}$$

with

$$N_{S,\parallel}(t) \equiv [1 + 2R_{SS}(t)] \cdot N_{SS}(t) + [1 + 2R_{SA}(t)] \cdot N_{SA}(t) \tag{18}$$

$$N_{A,\parallel}(t) \equiv [1 + 2R_{AS}(t)] \cdot N_{AS}(t) + [1 + 2R_{AA}(t)] \cdot N_{AA}(t) \tag{19}$$

$$N_{S,\perp}(t) \equiv [1 - R_{SS}(t)] \cdot N_{SS}(t) + [1 - R_{SA}(t)] \cdot N_{SA}(t) \tag{20}$$

$$N_{A,\perp}(t) \equiv [1 - R_{AS}(t)] \cdot N_{AS}(t) + [1 - R_{AA}(t)] \cdot N_{AA}(t) \tag{21}$$

where $N_{XY}(t)$ is population in state X that was initially pumped in state Y.

In this case we want to find the best *two* fitting spectra $\sigma_S(\nu)$ and $\sigma_A(\nu)$. We are helped by the fact that there are two separate and distinct DMA-H_2O data sets. We expand matrix equation (17) vertically to include in one equation both models and data sets. The models differ only in their initial conditions for the directly pumped populations, $N_{SS}(0)$ and $N_{AA}(0)$. Initial indirect populations $N_{SA}(0)$ and $N_{AS}(0)$ are zero by definition. From equation (17) it may be deduced that the normalization of either the initial populations or the cross-section of the two spectra is arbitrary to choose (only their product matters). This means that only the relative values of these initial populations are important and we may describe them by two fraction parameters (plus a scaling parameter between experiments):

$$N_{SS,pump\rightarrow S}(0) = f_S \tag{22}$$

$$N_{AA,pump\rightarrow S}(0) = 1 - f_S \tag{23}$$

$$N_{SS,pump\rightarrow A}(0) = r\,(1 - f_A) \tag{24}$$

$$N_{AA,pump\rightarrow A}(0) = r\,(f_A) \tag{25}$$

The values for f_S and f_A are the fractions for the directly pumped populations in levels 1_S and 1_A compared to the total excited population, for corresponding pump frequencies at modes S and A, respectively. The value for r is just a scaling parameter reflecting the ratio of total excited population between the two experiments, which will depend on relative pump intensity and cross-section.

We are then left with a total of 6 equations (isotropic, parallel and perpendicular for both experiments) to find the two spectra that best conform to data and model as a function of energy transfer and rotational diffusion rates.

F. Fit results

To avoid any influence of coherent artifacts on the modeling, we start the data analysis at 0.4 ps. For this time interval, all data is well described by the evolution of time-independent spectra, which indicates that the effects of spectral diffusion are negligible. Heating effects, caused by the shifting of absorption bands after decay and thermalization, were subtracted by an ingrowing end-spectrum (σ_{0^*}) which has the shape observed at 100 ps and time dynamics corresponding to the presented model.

The parameters entering the model are obtained by a global fitting routine that minimizes

$$\chi^2(par) = \sum_{\xi=1}^{3} \frac{[\Delta\alpha_{model}(t,\nu,par) - \Delta\alpha_{data}(t,\nu)]^2}{[\epsilon(\Delta\alpha_{data}(t,\nu))]^2} \tag{26}$$

as a function of parameters *par*. $\Delta\alpha_{data}(t,\nu)$ represents one of the three data sets of HDO and H_2O, with pump frequencies set at modes S and A, and $\epsilon(\Delta\alpha_{data}(t,\nu))$ are the respective standard deviation errors on this data set. $\Delta\alpha_{model}(t,\nu,par)$ represent the corresponding model defined by equations (9) through (25).

The results of the fits are shown in figures 4, 5, and 6. We find good simultaneous agreement between the data points and the fitted model (lines) for both the isotropic and anisotropic spectra. The cross section spectra for the S and A modes, shown in figure 9, have the expected shapes with a bleaching/stimulated emission and a red-shifted induced absorption. Furthermore the added $\nu = 0 \rightarrow 1$ transitions for modes S and A agree nicely with the linear spectrum, shown in figure 2.

The fitted anisotropies of the directly and indirectly pumped populations S and A, and that of population H, are shown in figure 10. These anisotropies, defined in equations (9) through (13), are used in equations (14) through (21) to construct the anisotropy dynamics shown in figures 4, 5, and 6. The directly pumped population in mode S (R_{SS}) shows a much faster anisotropy decay than the directly pumped population in mode A (R_{AA}). The anisotropies of the indirectly pumped population S and A (R_{SA} and R_{AS}) show an initial value of -0.2, corresponding to transfer over a 90° angle, and both decay with the same time constant as the whole complex (i.e. R_{AA}). This behavior is illustrated on the right hand side of figure 7 and follows from the fact that after transfer, the rotational diffusion D_M does not change the anisotropy for either case R_{SA} or R_{AS}: only D_C contributes. All curves are consistent with the proposed model of a fast rotation of the water molecule around the axis parallel to A (see fig. 1) and a slow reorientation of the DMA-water complex. As expected, the anisotropy decay curve of R_H is in between that of R_{SS} and R_{AA}.

All fit parameters are given in table I. The OH stretch mode in DMA-HDO decays with a time constant of $k_{ho^*}^{-1} = 1.8 \pm 0.2$ ps, which is about twice as long as that of the S mode in DMA-H_2O ($k_{so^*}^{-1}$) at 0.8 ± 0.1 ps. Direct decay of the A mode ($k_{ao^*}^{-1}$) is much slower and happens on timescales >15 ps. Transfer between the two normal modes (k_{sa}^{-1} and k_{as}^{-1}) happens at 0.8 ± 0.1 ps for S to A and slightly shorter, 0.7 ± 0.1 ps, for A to S. Dissipation of heat (k_{o^*o}) is found to be negligible in this experiment at timescales >100 ps.

With respect to the rotational diffusion, we find two very different timescales for the rotation of the water molecule within the complex and for the complex as a whole: $D_M^{-1} = 0.5 \pm 0.2$ ps and $D_C^{-1} = 7 \pm 1$ ps respectively. From the anisotropy end-levels, $R_{f,H}$ and $R_{f,SS}$, the standard deviation angle over which the water rotates within the complex ($\Delta\phi$) is determined to be $52 \pm 8\,^\circ$. This angle gives consistent end values for the anisotropies of these two modes.

For f_S and f_A we find values of 0.7 and 1, respectively, which implies that the A mode was exclusively excited when the pump was at A and that the excitation of the S mode lead to a $\sim 30\%$ excitation of mode A.

IV. DISCUSSION

A. Relaxation

For the vibrational lifetime of DMA-HDO we measure a time constant of 1.8 ± 0.2 ps. In the case of DMA-H_2O, we find that the vibrational excitation decays almost exclusively through the symmetric stretch normal mode ($k_{so^*} \gg k_{ao^*}$) with a time constant of 0.8±0.2 ps. To compare the vibrational lifetime of DMA-H_2O to that of DMA-HDO, we calculate the decay time of the (equilibrated) population S+A. In this way we find a time constant of 2.0 ± 0.2 ps for the vibrational relaxation of the OH oscillators in DMA-H_2O.

These findings can be explained if we consider the overtone of the bending mode as the principal accepting mode for these vibrations. We expect a favorable coupling between the overtone of the HOH bending mode and the S mode because they both possess the same symmetry. This is in contrast with the A mode, which possesses different symmetry and is also more separated in frequency from the bending mode overtone than the S mode. For the case of DMA-HDO we can think of the vibration as being composed of equal symmetric and asymmetric parts that only constructively interfere on the OH vibration (and destructively on the OD). Only the symmetric part of this vibration couples to the bending mode which is why the OH in HDO relaxes about two times slower than the pure S mode in DMA-H_2O.

We do not explicitly observe effects associated with mode-to-mode coupling between the bending mode and the symmetric stretching mode. The influence of this coupling in neat water has been studied by Lindner et al.[16] where it was found that excitation of the bending

mode leads to a blue shift of the associated OH-stretch frequency. However, this shift is small and in fact quite similar in nature to the effects associated with heating. In the current experiment it may therefore not be possible to distinguish between these two effects. In addition, the accumulation of population in the bending mode may be low because it rapidly relaxes to librations and other low-frequency modes.

The vibrational lifetimes we find for HDO (1.8 ± 0.2 ps) and H_2O (2.0 ± 0.2 ps) in DMA are both shorter than the value of 6.3±0.3 ps that was found in a previous study[17] on comparable systems of HDO-acetone and H_2O-acetone clusters in CCl_4. This difference in vibrational lifetime agrees with the notion that the frequency red-shift of the OH-stretch vibration of water-DMA (3450 cm^{-1}) is larger than that of water-acetone dissolved in CCl_4 (3520 cm^{-1}). For many hydrogen-bonded systems the vibrational lifetime T_1 can be related to the red-shift $\delta\nu_{OH}$ of the OH-stretch frequency relative to the gas phase frequency by[18,19]:

$$T_1 \propto (\delta\nu_{OH})^{-1.8} \tag{27}$$

There are several mechanisms that can account for the decrease of T_1 with increasing red-shift. In one mechanism, the decrease of T_1 is explained from the strengthening of the hydrogen-bond interaction. When the hydrogen bond gets stronger, the anharmonic coupling between this bond and the OH stretch vibration also increases, which leads to a faster relaxation, provided the hydrogen bond forms one of the accepting modes. The decrease of T_1 with increasing red-shift can also be caused by the decrease of the energy mismatch between the OH-stretch vibration and the overtone of the bending mode. For instance, in a theoretical study on the vibrational relaxation of HDO dissolved in D_2O it was shown that this effect causes the relaxation to become slower with increasing temperature[20].

Using expression (27), the lifetime of the OH-stretch vibration is expected to decrease by a factor of 2 going from water-acetone in CCl_4 to water-DMA, which is somewhat less than the observed factor of 3.3. This latter difference may find its origin in the fact that the water-acetone system is surrounded by an apolar solvent (CCl_4). The weak interaction with this solvent will frustrate an effective compensation of the energy mismatch between the OH stretch vibration and its main accepting mode(s) (e.g. the overtone of the bending mode), thus decelerating the relaxation.

B. Intramolecular energy transfer

Transfer between the two normal modes happens on timescales of 0.7±0.1 and 0.8±0.2 ps for $\nu = 1_S \rightarrow 1_A$ and $\nu = 1_A \rightarrow 1_S$, respectively. These transfer times are comparable to those found in the previously mentioned acetone-water study[17], where intramolecular transfer times were about 1 ps. The timescales in the water-acetone system were associated with the breaking and reforming of hydrogen bonds, converting between single and double hydrogen bound complexes. In this study, however, we do not observe a complete breaking of hydrogen bonds as reported in acetone, presumably because DMA forms more strongly bound hydrogen bond complexes than acetone. From the fact that we observe separate normal modes in the linear spectrum, which also fit with our pump-probe spectra (see fig. 2), we conclude that the two hydrogen bonds must be nearly equivalent for most molecules.

C. Rotational diffusion

The timescale we associate with reorientation of the complex, ($D_C^{-1} = 7 \pm 1$ ps), is similar to those reported in previous studies on water-acetone in CCl_4[11] (6.3±0.3 ps) and water-DMSO[13] (5 ps), although these reorientations were interpreted as being due to the water molecule alone. The rotational correlation time τ_r of a spherical particle in a solvent with viscosity μ_s may be approximated using the Stokes-Einstein-Debye equation:

$$\tau_r = \frac{\mu_s V}{k_B T} \tag{28}$$

where V is the solvated volume, k_B is the Boltzman constant and T the absolute temperature. From this equation, we expect the reorientation time of these complexes to be roughly proportional to the solvated volume times the viscosity of the surrounding solvent. DMA and DMSO have very similar viscosities (both $\mu_s \approx 2$ cP @ 25^oC) and from their respective molecular structures, we expect the solvated volume V of the DMSO complex to be slightly smaller than that of DMA. These values are consistent with the slightly faster rotational diffusion of DMSO compared to DMA. The water-acetone-CCl_4 system, unfortunately, can not be compared in this way because it is not clear what the size of the rotating water-acetone clusters is.

Besides the slow reorientation of the complex, we observe a much faster additional reorientation with a timescale $D_M^{-1} = 0.5 \pm 0.2$ ps. The fact that $D_C^{-1} \gg D_M^{-1}$ shows that

the system exhibits two very distinct rotations. As further confirmation, we find an angle of $\Delta\phi = 52 \pm 8\,^\circ$ that is consistent for the end-levels measured in *both* the OH-stretch in HDO and the symmetric stretch in H_2O. The magnitude of this angle implies that the water molecule in the DMA complex rotates approximately within a quarter circle around its hydrogen bonded equilibrium position. From this magnitude we may calculate with equation (B3) that the angular restoring force constant κ_M, exhibited by the hydrogen bonds, is approximately $5 \cdot 10^{-21}$ J rad^{-2}.

D. Implications

Several interesting properties of water in interaction with amide-like structures were measured that may help in the modeling of configurations involving water and amide groups (such as proteins). We see from our linear spectrum and indirectly from the measured anisotropic rotational diffusion rates that the water molecules in this experiment form hydrogen bond connections on both sides to DMA molecules. Furthermore, the red-shifted OH frequency of water in DMA indicates that these hydrogen bonds are relatively strong compared to for example water in acetone. This suggests that water can act as a sort of extension cord, creating hydrogen bond connections between different amide groups that could otherwise be sterically hindered. This study quantifies experimentally the limited range of motion (in a quarter circle) that the water molecule exhibits in such connections. It is clear that this water connection is not cylindrically symmetric but has a certain directional preference, likely such that the oxygen and hydrogen atoms partaking in either of the hydrogen bonds (O-H$\cdots$O) lie on a single line in the direction of a lone pair on the oxygen of DMA. This means that the rearrangement of amide groups connected by a water molecule has to involve also the appropriate directional reorientation of the connecting C=O groups. An important consequence is that the protein-water chain will exhibit very specific structural rigidity.

V. CONCLUSION

We have studied the energy transfer and reorientational dynamics of water, hydrogen bonded in a complex of two DMA molecules, using polarization-resolved mid-infrared spec-

troscopy. We found that the vibrational energy relaxation for H_2O occurs mainly via the symmetric stretch normal mode with a time constant of 0.8 ± 0.2 ps. The relaxation of the equilibrated symmetric and asymmetric normal modes in DMA-H_2O was found to occur with a time constant of 2.0 ± 0.2 ps which is comparable to the relaxation time found for the OH vibration in HDO (1.8 ± 0.2 ps). We attributed these findings to a favorable coupling between the symmetric stretch normal mode and the overtone of the bending mode in H_2O. For the energy transfer *between* the symmetric and asymmetric normal modes in H_2O we found time constants of 0.8 ± 0.1 and 0.7 ± 0.1 ps, which we associated with fluctuations in the hydrogen bond strength between the water and DMA complex. Rotational diffusion of water in DMA was found to be mainly limited to hinging motions over an angle of $52 \pm 8\,^\circ$ around the connecting hydrogen bonds on a timescale of 0.5 ± 0.2 ps. Additionally, an overall reorientation time of 7 ± 1 ps was found and associated with rotational diffusion of the water-DMA complex as a whole. The measured properties of water in interaction with amide-like structures can help in the understanding of its role in processes such as the folding of proteins.

Acknowledgments

This work is part of the research program of the Foundation for Fundamental Research on Matter (FOM) which is financially supported by the Dutch organization for Scientific Research (NWO). The authors thank Hinco Schoenmaker for his technical support and Mischa Bonn for helpful comments on this manuscript.

APPENDIX A: SOLVING A SYSTEM OF FIRST ORDER, LINEAR ODES

We solve the system of first order, linear ordinary differential equations (ODEs)

$$\frac{d}{dt}\,\vec{x}\,(t) = A\,\vec{x}\,(t) \tag{A1}$$

for vector $\vec{x}\,(t)$ as a function of t. From the *eigenvalues* of A we construct a diagonal matrix D and from the *eigenvectors* of A we construct a matrix V, such that the following equation holds:

$$A\,V = V\,D \tag{A2}$$

We use matrix V to construct a new vector $\vec{y}\,(t)$ such that

$$\vec{x}\,(t) = V\,\vec{y}\,(t) \tag{A3}$$

We can now diagonalize the original problem:

$$\frac{d}{dt}\,\vec{x}\,(t) \;=\; \frac{d}{dt}\,(V\vec{y}\,(t)) = A\,(V\vec{y}\,(t)) = V D\,\vec{y}\,(t) \tag{A4}$$

$$\Rightarrow \frac{d}{dt}\,\vec{y}\,(t) \;=\; D\,\vec{y}\,(t) \tag{A5}$$

The set of equations, $\vec{y}\,(t)$, can be solved straightforwardly (because D is diagonal):

$$\vec{y}(t) \;=\; \exp(D\,t)\;\vec{y}\,(0) \;=\; \exp(D\,t)\,V^{-1}\,x\,(0) \tag{A6}$$

Finally we can transform the obtained solution for $\vec{y}\,(t)$ back to $\vec{x}\,(t)$ with equation A3:

$$\vec{x}\,(t) = V\exp(D\,t)\;V^{-1}\,\vec{x}\,(0) \tag{A7}$$

APPENDIX B: ANISOTROPY END-LEVELS

We determine the anisotropy end-levels $R_{f,H}$ and $R_{f,SS}$ as a function of the angular distribution over the partial circle shown in figure 7. We assume that the water molecule experiences a restoring force proportional to the displacement angle ϕ from its equilibrium position:

$$F_M = -\kappa_M \phi \tag{B1}$$

with F_M the molecular restoring force and κ_M the associated force constant. This force may be equivalently described by the potential

$$V_M = -\int F_M d\phi = \frac{1}{2}\kappa_M \phi^2 \tag{B2}$$

which, using Boltzman statistics, leads to a gaussian distribution:

$$\rho_M = \exp(-V_M/k_B T) \equiv \exp(-\phi^2/2(\Delta\phi)^2) \tag{B3}$$

where we implicitly define $\Delta\phi = \sqrt{k_B T/\kappa_M}$ as the standard deviation angle of the distribution. The Boltzman constant, k_B, is valued $1.38 \cdot 10^{-23}$ J K^{-1} and T is the absolute temperature.

We now evaluate equation (4) for $t \to \infty$ by integrating over all possible end states that are weighed with probability distribution ρ_M:

$$R(t \to \infty) = \frac{2}{5}\langle P_2(\hat{\mu}(0) \cdot \hat{\mu}(\infty)\rangle \tag{B4}$$

$$= \frac{\int_{-\pi}^{\pi} \rho_M \left[3/5(\hat{\mu}(0) \cdot \hat{\mu}(\phi))^2 - 1/5\right] d\phi}{\int_{-\pi}^{\pi} \rho_M \, d\phi} \tag{B5}$$

The last line contains the inner product between the transition dipole moments as a function of angle ϕ. This angle ϕ is defined as the angle over which the water molecule is rotated within the complex (around the axis parallel to mode A). As the water molecule rotates, so do the transition dipole moments for modes H and S (but not of A). Both these rotations can be parameterized as a function of angle ϕ using a cone with half angle α. This angle α is equal to the angle between the direction of the transition dipole moments $\hat{\mu}(\phi)$ and the axis around which it rotates (i.e. the direction of mode A). From the geometric properties of the water molecule we find that for mode H this angle is 38 degrees and for mode S it is 90 degrees. Finally, we project the unit vectors $\hat{\mu}(\phi))$ and $\hat{\mu}(0)$ (which both lie on the surface of the cone) onto each other, and derive the following expression for the inner product:

$$\hat{\mu}(0) \cdot \hat{\mu}(\phi) = \cos^2(\alpha) + [1 - \cos^2(\alpha)] \cos(\phi) \tag{B6}$$

This expression is substituted into equation (B5) using $\alpha = 38^\circ$ and $\alpha = 90^\circ$ to find values for $R_{f,H}$ and $R_{f,SS}$, respectively. The integration was performed numerically as a function of parameter $\Delta\phi$ to yield the corresponding values for $R_{f,H}$ and $R_{f,SS}$ that best fit the data.

* Electronic address: r.timmer@amolf.nl

[1] O. F. Mohammed, D. Pines, J. Dreyer, E. Pines, and E. T. J. Nibbering, Science **310**, 83 (2005).

[2] E. Meyer, Protein Science **1**, 1543 (1992).

[3] S. K. Pal, J. Peon, B. Baghi, and A. H. Zewail, J. Phys. Chem. B **106**, 12376 (2002).

[4] S. K. Pal and A. H. Zewail, Chem. Rev. **104**, 2099 (2004).

[5] J. D. Eaves, J. J. Loparo, C. J. Fecko, S. T. Roberts, A. Tokmakoff, and P. L. Geissler, Proc. Natl. Acad. Sci. U.S.A **102**, 13019 (2005).

[6] T. Steinel, J. B. Asbury, J. Zheng, and M. D. Fayer, J. Phys. Chem. A **108**, 10957 (2004).

[7] G. Gallot, S. Bratos, S. Pommeret, N. Lascoux, J. C. Leicknam, M. Kozinski, W. Amir, and G. M. Gale, J. Chem. Phys. **117**, 11301 (2002).

[8] J. Stenger, D. Madsen, P. Hamm, E. T. J. Nibbering, and T. Elsaesser, Phys. Rev. Lett. **87**, 027401 (2001).

[9] H.-K. Nienhuys, R. A. Van Santen, and H. J. Bakker, J. Chem. Phys. **112**, 8487 (2000).

[10] H. Graener, G. Seifert, and A. Laubereau, Chemical Physics **175**, 193 (1993).

[11] J. J. Gilijamse, A. J. Lock, and H. J. Bakker, PNAS **102**, 3202 (2004).

[12] D. Cringus, S. Yeremenko, M. S. Pshenichnikov, and D. A. Wiersma, J. Phys. Chem. B **108**, 10376 (2004).

[13] A. Wulf and R. Ludwig, ChemPhysChem **7**, 266 (2006).

[14] Y. L. A. Rezus and H. J. Bakker, PNAS **103**, 18417 (2006).

[15] T. Takamuku, D. Matsuo, M. Tabata, T. Yamaguchi, and N. Nishi, J. Phys. Chem. B **107**, 6070 (2003).

[16] J. Lindner, P. Vöhringer, M. S. Pshenichnikov, D. Cringus, D. A. Wiersma, and M. Mostovoy, Chem. Phys. Lett. **421**, 329 (2006).

[17] H. J. Bakker, J. J. Gillijamse, and A. J. Lock, ChemPhysChem **6**, 1146 (2005).

[18] R. E. Miller, Science **240**, 447 (1988).

[19] S. Woutersen, U. Emmerichs, H.-K. Nienhuys, and H. J. Bakker, Phys. Rev. Lett. **81**, 1106 (1998).

[20] C. P. Lawrence and J. L. Skinner, J. Chem. Phys. **119**, 3840 (2003).

par	value	*par*	value
$k_{ho^*}^{-1}$	1.8 ± 0.2 ps	D_M^{-1}	0.5 ± 0.2 ps
k_{sa}^{-1}	0.8 ± 0.1 ps	D_C^{-1}	7 ± 1 ps
k_{as}^{-1}	0.7 ± 0.1 ps	$\Delta\phi$	52 ± 8 °
$k_{so^*}^{-1}$	0.8 ± 0.2 ps	f_S	0.69 ± 0.08
$k_{ao^*}^{-1}$	>15 ps	f_A	1.01 ± 0.06
$k_{o^*o}^{-1}$	>100 ps		

TABLE I: Fit parameters of the model, explained in the text.

LIST OF FIGURES

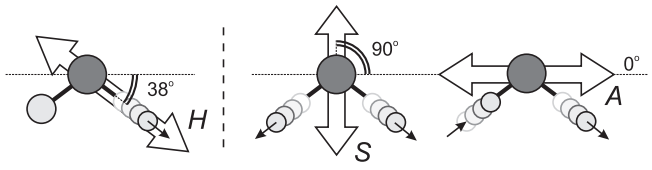

FIG. 1: OH-stretching mode in HDO (left) and symmetric and asymmetric stretching modes in H_2O (middle and right). The big white arrows indicate the directions of the transition dipole moments and the small black arrows indicate the shifting of the hydrogen atoms.

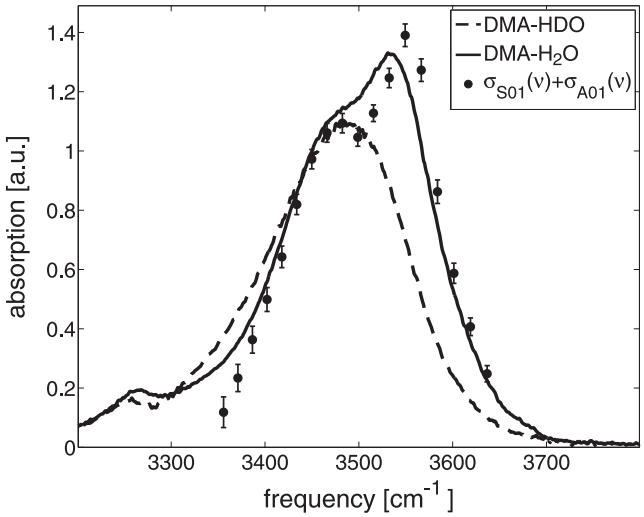

FIG. 2: Linear absorption spectra of DMA-HDO and DMA-H_2O (mentioned in text), with their reference solvents subtracted. Also shown are the added $\nu = 0 \rightarrow 1$ spectra of $\sigma_S(\nu)$ and $\sigma_A(\nu)$ resulting from the global fit.

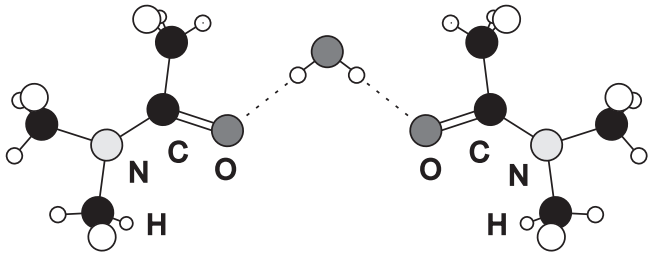

FIG. 3: DMA-water complex: each water molecule is hydrogen bonded on either side to the oxygen atom of a DMA molecule.

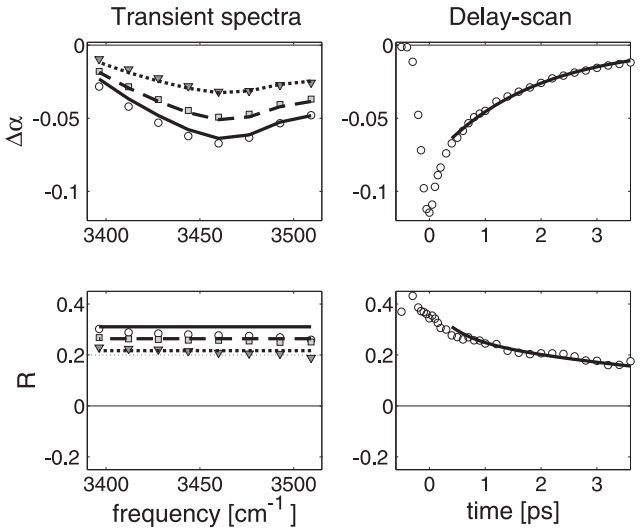

FIG. 4: Left: isotropic (top) and anisotropic (bottom) transient spectra for HDO. The circles, squares and triangles are data points at pump-probe delays of 0.4, 0.8 and 1.6 ps, respectively. The solid, dashed and dotted lines are respective evaluations of the fitted model, described in the text, at these same times. Right: Delay-scan of the isotropic (top) and anisotropic (bottom) signal at 3460 cm^{-1}, circles are the data points and the line results from the fitted model.

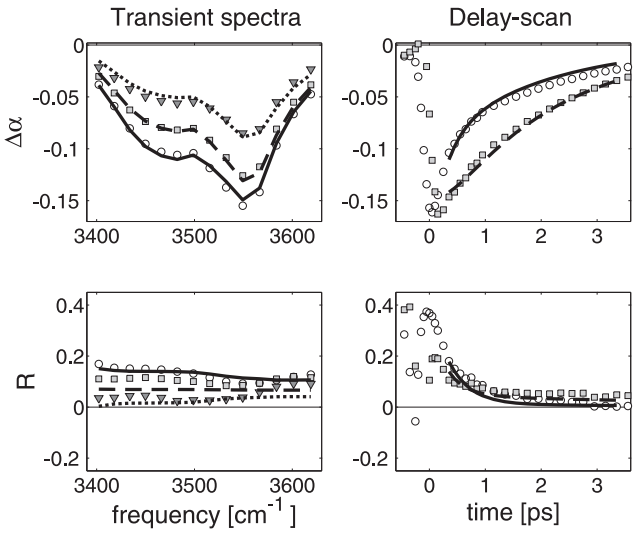

FIG. 5: Left: isotropic (top) and anisotropic (bottom) transient spectra for H_2O where the pump frequency was set to 3450 cm^{-1} (resonant with the symmetric OH stretch frequency). The circles, squares and triangles are data points of the absorption changes at pump-probe delays of 0.4, 0.8 and 1.6 ps, respectively. The solid, dashed and dotted lines are respective evaluations of the fitted model, described in the text, at these same times. Right: delay-scans of the isotropic (top) and anisotropic (bottom) signal at two frequencies. The circles and squares correspond to data points at 3450 and 3550 cm^{-1}, respectively. The solid and dashed lines are respective evaluations of the fitted model at these same frequencies.

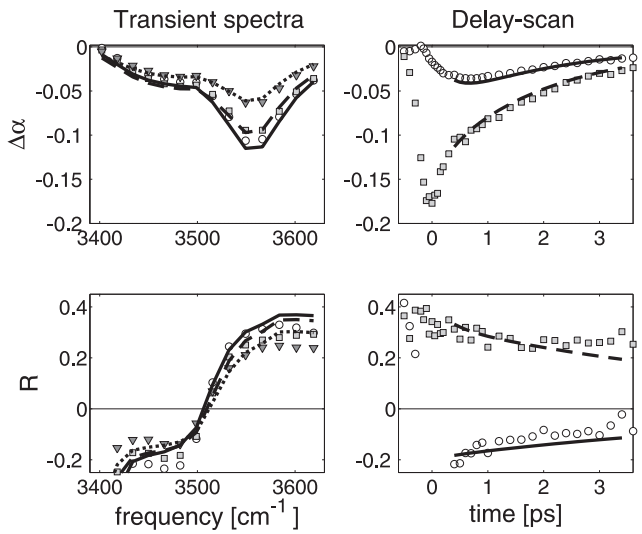

FIG. 6: Same as figure 5 but with the pump frequency set at 3550 cm^{-1} (resonant with the asymmetric OH stretch frequency)

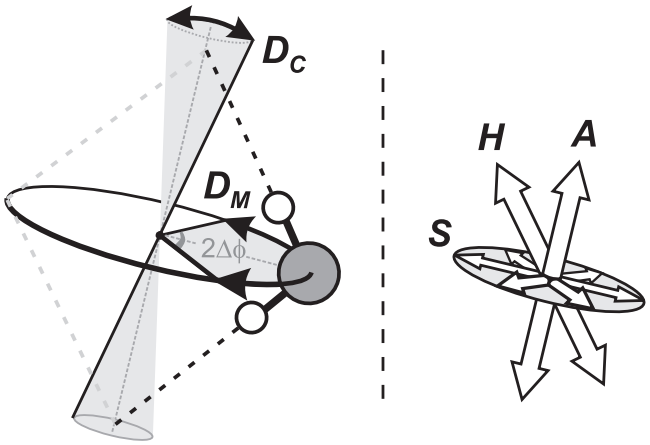

FIG. 7: Left: Motion of the water molecule is split into two rotational diffusions: molecular rotations on a (partial) circle perpendicular to the transition dipole moment of A and rotations of the whole complex that spread out in a cone around it. Right: Transfer from mode S to A and vice versa is over 90° and so always into a plane perpendicular to the excitation. Subsequent rotations in this plane do not change the anisotropy further. The initial direction of mode H is shown for comparison.

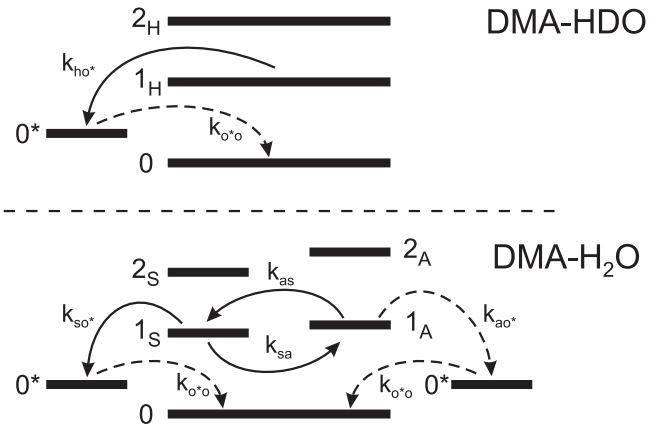

FIG. 8: Energy level diagrams showing the transfer rates between levels. The top diagram shows DMA-HDO and the bottom one DMA-H_2O. Dashed arrows indicate relatively slow processes for the experiments discussed in this work.

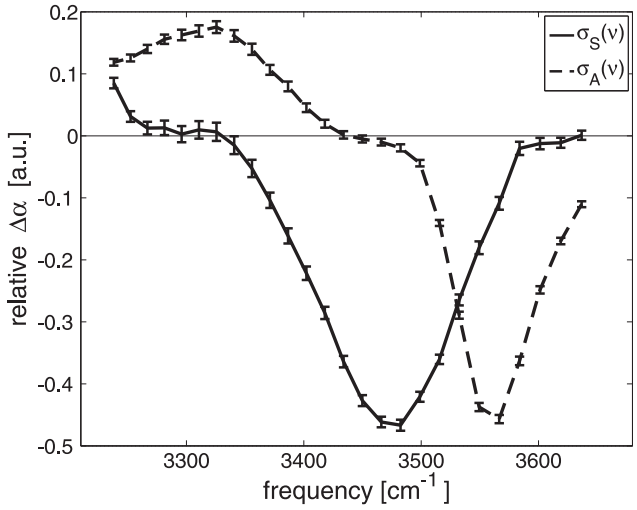

FIG. 9: Decomposed spectra of the relative absorption changes corresponding to the symmetric and asymmetric OH stretch vibrations at measured frequencies. Solid and dashed lines are used, as a guide to the eye, to connect these points for S and A, respectively.

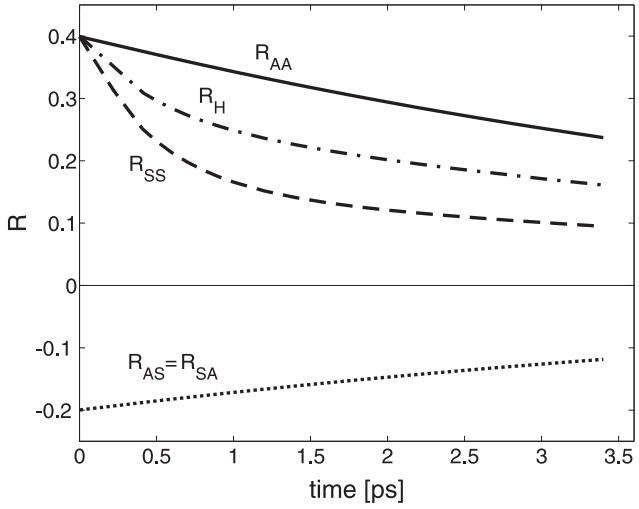

FIG. 10: Fitted anisotropy curves of mode H in DMA-HDO and of the directly and indirectly pumped populations S and A in DMA-H_2O, described in the text and used in the anisotropic parts of figures 4, 5, 6.